Uncertainty evaluation for velocity–area methods

J. Steinbock [a],*, A. Weissenbrunner [a], M. Juling [a], T. Lederer [a], P.U. Thamsen [b]

[a] *Physikalisch-Technische Bundesanstalt (PTB), Abbestr. 2-12, 10587 Berlin, Germany*
[b] *Technische Universität Berlin, Department of Fluid System Dynamics, Straße des 17. Juni 135, 10623 Berlin, Germany*

ARTICLE INFO

ABSTRACT

Velocity–area methods are used for flow rate calculation in various industries. Applied within a fully turbulent flow regime, modest uncertainties can be expected. If the flow profile cannot be described as "log-like", the recommended measurement positions and integration techniques exhibit larger errors. To reduce these errors, an adapted measurement scheme is proposed. The velocity field inside a Venturi contour is simulated using computational fluid dynamics and validated using laser Doppler anemometry. An analytical formulation for the Reynolds number dependence of the profile is derived. By assuming an analytical velocity profile, an uncertainty evaluation for the flow rate calculation is performed according to the "Guide to the expression of uncertainty in measurement". The overall uncertainty of the flow rate inside the Venturi contour is determined to be 0.5% compared to $\approx$0.67% for a fully developed turbulent flow.

1. Introduction

Flow measuring devices can be grouped into three main categories: integrative methods like differential pressure measurements or magnetic inductive devices, semi-integrative methods like ultrasonic path meters, and sampling based techniques which rely on a discrete number of measurement positions such as velocity–area methods.

These methods have been successfully applied to a variety of flow conditions. Especially for larger pipes, open field acceptance tests or temporary measurements, they present a feasible alternative to conventional flow measuring devices. Another advantage is that these methods can easily be applied within an arbitrary measurement section or open channel flow. Though traditionally used with pitot tubes or inserted devices, they can also be applied to optical velocity measurement techniques like laser Doppler anemometry (LDA).

In order to convert the pointwise velocities to a flow rate, a precise numerical integration method is preferable. The overall idea is to get an acceptable uncertainty for the flow rate with the least possible number of sample positions. The most general formulation of the measurement problem is: $Q = \int_0^R \int_0^{2\pi} v \cdot r \, d\varphi \, dr$. For the case of a rotational symmetric turbulent pipe flow in a circular measurement section the problem is reduced to a path

integration: $Q = 2\pi \int_0^R r \cdot v \, dr$. For a known velocity profile the metrological effort can be even further reduced from a path measurement to a single point measurement. Aichelen [1] proposed placing the probe at the position where the volumetric flow velocity occurs. The point of the average velocity varies for different models of turbulent pipe flow depending on the Reynolds number, as shown in Fig. 1. A different approach is to measure the centreline velocity while computing the flow rate using a calibration factor as proposed by Strunck et al. [11]. However, by restricting the measurement of an unknown profile to just one point, there is no way to tell whether the implicit assumptions concerning the shape of the profile are viable. Therefore, in general multiple radial positions are necessary. Quite a few integration techniques and guidelines for optimized measurement positions have been published. Based on Winternitz and Fischl [15] the commonly used integration procedures are described in the standards ISO 3354 [3], ISO 3966 [4] and VDI 2640 [12]. These methods are based on the assumption of a fully developed turbulent pipe flow where the velocity can be described by "log-like" behavior. This can only be achieved by a long undisturbed entrance length or flow conditioning both are often not feasible. The *true* velocity field in the measuring plane is therefore in general unknown, thus making the uncertainty evaluation of the standard methods quite cumbersome.

In order to create well-defined conditions, a Venturi contour is investigated. Due to the different shapes of the velocity distribution in the Venturi nozzle, it will be shown that the standard velocity–area methods exhibit higher errors. To reduce the uncertainty for the flow rate calculation, optimized measurement
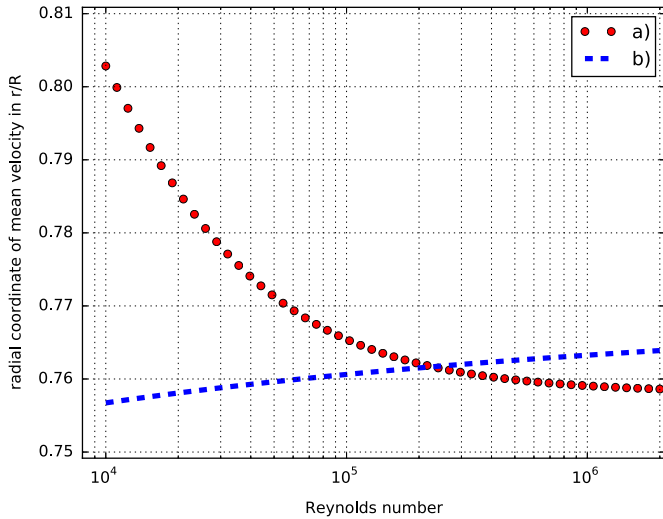
Fig. 1. Radial location of the average velocity: (a) Gersten/Herwig profile acc. to [8], (b) power-law profile acc. to Miller [9].

Fig. 2. Discretization error of velocity–area methods applied to the Gersten/Herwig profile $(k = 1)$; log linear (LL), log Chebyshev (LC), centroid (C) and centroid with wall correction (CW).

positions are derived. To compare the performance of the new method, an uncertainty evaluation based on analytical velocity profiles is applied. We consider the fully turbulent pipe flow first, since the descriptions of the uncertainties in the standards are rather short.

2. Uncertainty evaluation for fully developed turbulent pipe flow

Velocity–area methods calculate the flow rate as follows: the cross section is divided into equally sized parts. The measurement position for each piece is given either by the centroid or the position of the average velocity in this area. The flow rate is determined as the mean measured velocity multiplied with the area of the cross section. Some integration techniques apply an extrapolation procedure/a wall correction. Recommended locations for up to five radial sample positions are tabulated in the standards ISO 3354 [3], ISO 3966 [4] and VDI 2640 [12]. These procedures, developed to cope with only limited access to data processing and automation, are log linear (LL), log Chebyshev (LC), centroid (C), and centroid with wall correction (CW). Due to the pointwise sampling of the continuous velocity field, an intrinsic discretization error must be taken into account. To assess this error, an analytical reference profile with known flow rate is required. It is mandatory that this profile conveys the essential geometric and hydraulic phenomena of the emulated flow. A generic velocity formulation according to Gersten and Herwig [8] is used for the investigation of the discretization error. This profile, referred to as the GH profile, is a closed formulation for the streamwise velocity component of a flow in a round pipe. The pipe flow model is valid in the fully turbulent range for Reynolds numbers between 4×10^4 and 1×10^7.

All methods were analyzed for the recommended five radial sample positions. The derived flow rate was then compared to the exact integration of the GH profile. This procedure is performed for a Reynolds number range of 1×10^4–2×10^6. All methods show a Reynolds number dependence. It is worth noting that despite measuring on only five radial sample positions, even the highest discretization error is smaller than 2%. For the LL and LC, the errors are smaller than 0.6% compare Fig. 2.

To point out the importance of the discretization error, the overall uncertainty has to be derived. Neglecting any radial asymmetries, a minimal measurement uncertainty can be established based on the discretization error, the accuracy of the
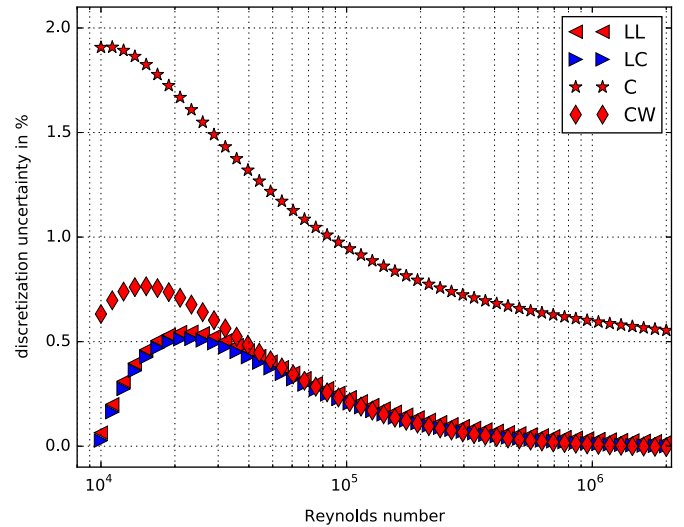
traverse system, the uncertainty of the velocity measurement and the uncertainty of the cross-sectional area.

The influence of the accuracy of the traverse system on the measurement positions and its effect on the uncertainty of the flow rate are determined as follows. The sensitivity coefficient for each individual measurement position is estimated by a numerical differential quotient as proposed in the "Guide to the expression of uncertainty in measurement (GUM)" [5]. Each emulated measurement is repeated with slightly shifted sample positions. For the sake of simplicity all measurement positions are confined to a dimensionless radial coordinate r/R between 0 and 1. If for any shifted sample position a radial coordinate outside of the conduit occurs, it is mirrored either on the wall or on the centreline. Furthermore, it is assumed that all positional errors are uncorrelated and of the same magnitude. In ISO standard 3966 [4] a maximum permissible positional error of 0.5% pipe diameter D is given. The following configurations will be discussed: $\Delta r/R = 0.50\%$ D, 0.25% D, 0.1%D and 0.05%D. For large Reynolds numbers the influence of the positioning precision declines. This is due to the rather flat velocity profile. The effect of the steeper curvature in the proximity of the wall cannot be sampled by the (recommended) five measurement positions. The uncertainty contribution of the other velocity–area methods is of the same order. The resulting traverse uncertainties for the log Chebyshev method are shown in Fig. 3.

As an example, the uncertainty of the log Chebyshev method at a Reynolds number of 1×10^5 is presented. Fig. 2 yields the discretization uncertainty with 0.21%. Fig. 3 yields the positioning contribution for an uncertainty of 0.1%D with 0.1%. The uncertainty of the velocity measurement, based on laser Doppler anemometry, is estimated to be 0.2%. The uncertainty of the cross section's diameter, nominally 75 mm, is 0.03 mm thus accounting for an uncertainty of the flow area of 0.1%.

The combined standard uncertainty for the log Chebyshev method can be stated to be 0.32% $(k=1)$ or 0.65% $(k=2)$ for this particular configuration, as shown in Table 1, column 1. For a different measurement setup, e.g. a different velocity uncertainty, these values can be easily adapted.

The example of the uncertainty assessment shows that the discretization error accounts for 40% of the overall uncertainty. It is obvious that with an increased number of sample positions, the intrinsic discretization error can be reduced. Depending on the application, the proper ratio between measuring time and accuracy has to be weighed.
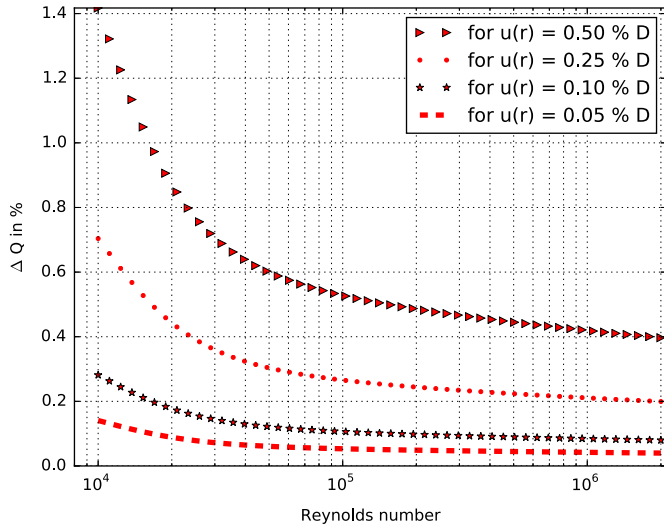
Fig. 3. Influence of the positional accuracy on the determined flow rate for the log Chebyshev method applied to the Gersten/Herwig velocity profile $(k = 1)$.

Table 1
Uncertainty of velocity–area methods for *Re* 1.0×10^5.

Profile	GH	Tanh	
Procedure	LC	LC	Opt
Discretization uncertainty	0.210	0.530	0.070 (%)
Positional uncertainty	0.100	0.045	0.067 (%)
Velocity uncertainty	0.200	0.200	0.200 (%)
Area uncertainty	0.100	0.100	0.100 (%)
Combined variance	0.1041	0.3309	0.059
Comb. uncertainty $(k = 1)$	0.32	0.58	0.24 (%)
Comb. uncertainty $(k = 2)$	0.65	1.15	0.49 (%)

3. Uncertainty evaluation for flow rate determination inside a Venturi contour

A fully developed turbulent flow cannot be realized on most occasions. Constrictions and nozzles can therefore be applied to homogenize the velocity profile. In the new high temperature water flow standard at the Physikalisch-Technische Bundesanstalt (PTB) in Berlin, a Venturi nozzle with a diameter ratio of 0.5 is used, see Fig. 4. The form of the radial velocity distribution can no longer be described with the commonly accepted log law. In its place an analytical tanh profile is applied as proposed by Strunck et al. [11]. The formula for the velocity profile inside the Venturi contour is represented by:

$$u_{tanh}(r) = u_0 \tanh\left(k\left(1 - \frac{r}{R}\right)\right)^b \tag{1}$$

where u_0 represents the dimensionless maximum velocity, k is the displacement parameter and b denotes the form parameter. All three coefficients generally depend on the particular geometry of the Venturi nozzle and the Reynolds number. To determine these parameters, laser Doppler measurements as well as computational fluid dynamic (CFD) simulations were conducted. The Reynolds numbers 1×10^5, 3×10^5, 4.5×10^5 and 1×10^6, relating to an inlet diameter D of 150 mm were considered.

3.1. Experimental setup

A 6 m measuring section of nominal diameter D150 mm was installed at the German standard for the scale "thermal energy". The flow standard, described by Mathies [7], is capable of flow rates between $3\ \mathrm{m^3h^{-1}}$ and $1000\ \mathrm{m^3h^{-1}}$ while maintaining temperatures from $3\ ^\circ\mathrm{C}$ to $90\ ^\circ\mathrm{C}$. The uncertainty of the re-presented flow is rated at 0.04% $(k = 2)$. This uncertainty is reached via a traceable gravimetric system. The temperature uncertainty is 50 mK. In the middle of the measuring section a Venturi nozzle (short form) [2] featuring a throat diameter of 75 mm is placed. The relevant metrological Venturi contour is designed as an insert. A rugged industrial armature made by *Noris Armaturen GmbH* with meta-glass windows is employed as a pressure containment. The Venturi throat is equipped with a precision glass tube, thus allowing laser Doppler measurements to be performed inside the constriction. A positioning system moves the active laser Doppler measuring volume throughout the whole cross section. A ray tracing method is applied to compute the measurement positions. The laser probe is a Nd:YAG 1D system with a rated power of 200 mW and a wavelength of 532 mm from *ILA GmbH*. To reach the projected Reynolds numbers, different combinations of flow rate and temperature were employed. Each profile was measured with an angular resolution of 10° at 21 radial sample positions.
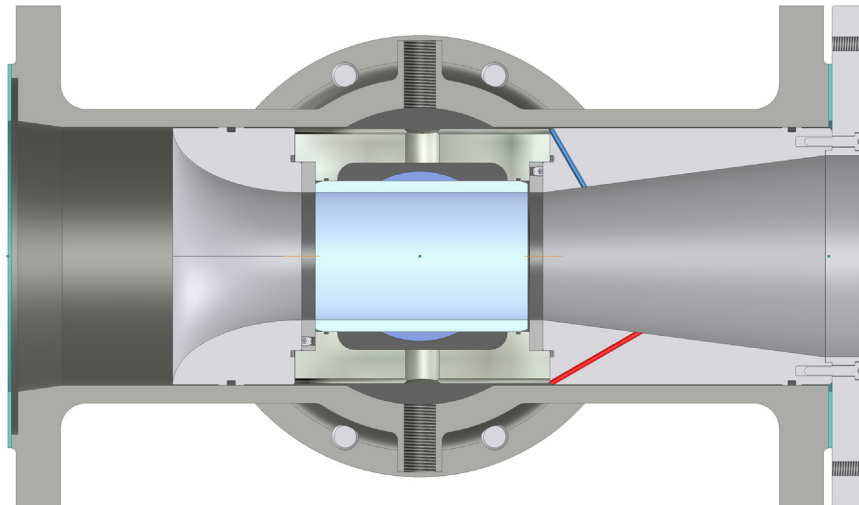

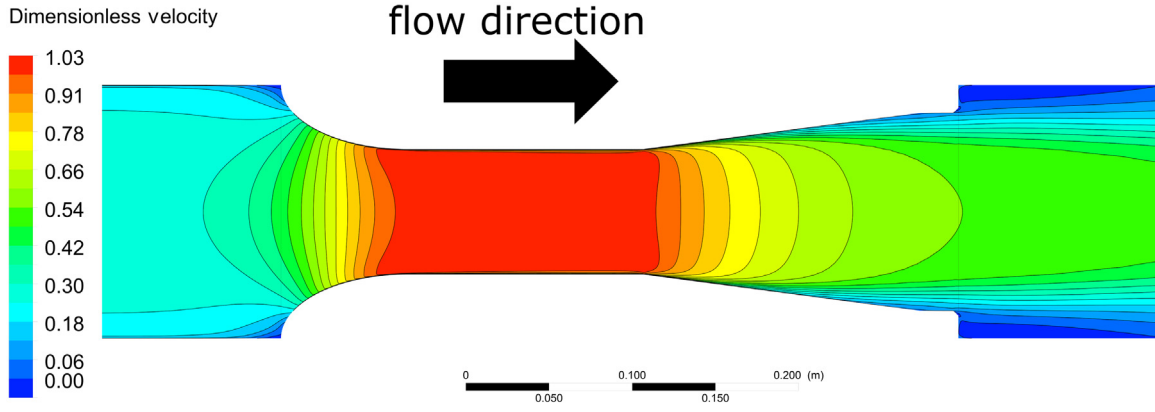**Fig. 4.** Sectional view of the CAD model of the Venturi contour.

Fig. 5. Contour plot of the simulated dimensionless axial velocity distribution on the middle plane at a Reynolds number of 3×10^5.
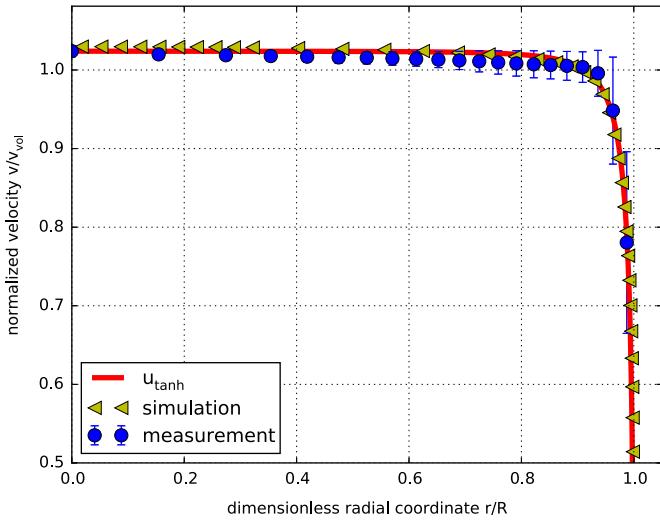

Fig. 6. The fitted tanh function, measurement and simulation data predicting the velocity profile inside the Venturi nozzle for $Re = 3e5$.

3.2. Numerical setup

The numerical simulations are performed with the commercial CFD code CFX from Ansys. A structural hexa mesh is generated with about 5×10^6 grid points, where the dimensionless wall distance of the first node is $y^+ \approx 1$. For the boundary conditions, a hydraulic smooth no-slip wall is chosen along with a fully developed flow profile from earlier simulations with the same Reynolds numbers for the inlet. An average pressure is set at the outlet. The Wilcox-$\kappa - \omega$ turbulence model [14] is employed, as it yields the best performance for turbulent pipe flow simulations, compare Weissenbrunner et al. [13]. As expected, the flow profile inside the constriction is flatter than the fully developed profile, see Fig. 5. At the end of the exit cone flow separation occurs. The simulation shows the transient behavior of the separation. Nevertheless, the velocity field in the measuring section is not affected by this detachment.

3.3. Analytical profile

The coefficients of $u_{tanh}(r)$ from Eq. (1) are calculated by fitting the parameters to the measurement data. The python fit routine *scipy.optimize.fmin* is used, which is based on the downhill simplex algorithm by Nelder [10]. As fit criteria the integral

$$\varepsilon = \min_{u_0, k, b} \left(\left(\int_0^1 (u_{tanh}(r) - u_{meas}(r))^2 r \, dr \right)^{1/2} \right) \tag{2}$$

is considered, where $u_{meas}(r)$ represents the measurement. The integral is solved by interpolating $u_{meas}(r)$ and $u_{tanh}(r)$ between the discrete measurement points with piecewise linear functions. The error ε between the fitted profile and the measurements is in the range 1.2–1.5%. The results of the measurement, the simulation and the fitted profile inside the Venturi nozzle at a Reynolds number of 3×10^5 are shown in Fig. 6. The error bars at the measurement values represent the measured axial turbulence in %. Qualitatively all three profiles show satisfying agreement. The simulated results exhibit slightly higher dependences of the Reynolds number than the measurement profiles. One explanation for the generally low Reynolds influence can be found in the flow coefficient: it is just dependent on the geometric dimensions [2]. Thus, the implemented Venturi contour is convenient for flow conditioning. It is worth noting that other nozzle types, for example the ISA-1932, also exhibit a low Reynolds dependence. Its coefficient changes by about 0.4% for this Reynolds range. To perform the same studies for the tanh profile as for the fully developed Gersten/Herwig profile, a prediction of the Reynolds number dependence of the coefficients was necessary. A set of linear functions was fitted to the parameters u_{0i}, k_i, and b_i. The coefficients within a Reynolds number range of $1 \times 10^5 - 1 \times 10^6$ can then be formulated as follows:

$$u_0(Re) = - 3.781 \times 10^{-9} \cdot Re + 1.0250$$
$$k(Re) = 1.418 \times 10^{-6} \cdot Re + 5.3150$$
$$b(Re) = 4.629 \times 10^{-8} \cdot Re + 0.3806. \tag{3}$$

3.4. Uncertainty for improved tanh method

For further uncertainty assessment the velocity–area methods were tested against the analytical tanh nozzle profile. All velocity–area methods exhibit a slightly Reynolds dependent discretization error in the range of 0.5% to 1.2%, as illustrated in Fig. 7. Due to the flat top velocity distribution, the obtained positional uncertainties are smaller than for the fully turbulent flow, compare Section 2. Furthermore there is only a marginal influence of the Reynolds number since the change in the slope of the velocity profile cannot be covered by only five sample positions. Taking the same assumptions into consideration as before, the overall uncertainty can now be stated as 1.15%, compare Table 1, column 2. This is almost double the value as for the fully developed flow. From this rise in uncertainty it can be concluded that for non-log-like velocity profiles an adapted integration method has to be applied.
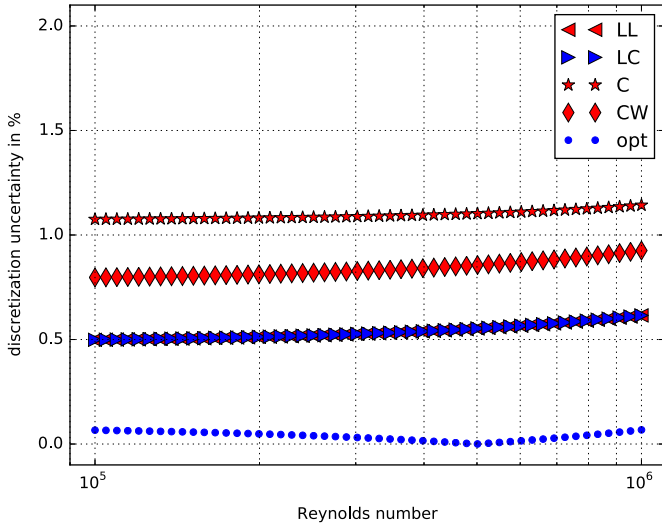
Fig. 7. Discretization error of velocity–area methods applied to the tanh profile ($k = 1$); log linear (LL), log Chebyshev (LC), centroid (C), centroid with wall correction (CW) and optimized (opt).
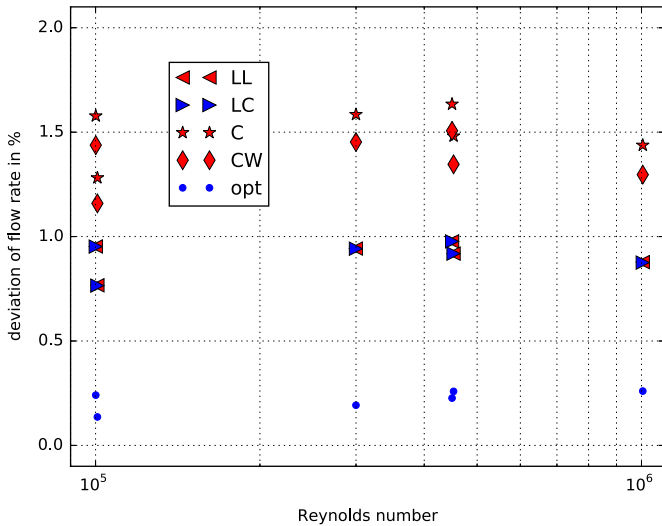

Fig. 8. Deviation of flow rates obtained by different velocity–area methods compared to a gravimetric flow standard; log linear (LL), log Chebyshev (LC), centroid (C), centroid with wall correction (CW) and optimized (opt).

Otherwise, higher uncertainties have to be accepted even if the measuring conditions are favorable due to the homogenization of the flow in the constriction.

To apply the velocity–area procedure to this specific flow situation, new sample positions are required. The cross section is therefore divided into subsections of equal area. Five radial subsections are chosen to be comparable to common velocity–area methods. For each subsection the radial position of the mean velocity is computed. For a known radial velocity distribution it is always possible to find (Reynolds) optimized sample positions so that the discretization error is negligible. To cover the Reynolds number range $1 \times 10^5 - 1 \times 10^6$, we choose optimized points for a Reynolds number of 5×10^5. For the proposed tanh profile, the discretization error can be reduced to a maximum of 0.07%, compare Fig. 7. The optimized sample positions are $r/R = 0.3311$, 0.5577, 0.7159, 0.8466 and 0.9706. The reduced uncertainty can then be stated as 0.24% ($k = 1$) or 0.49% ($k = 2$), compare Table 1, column 3. It is obvious that the discretization error is only a marginal part of the combined uncertainty. For further uncertainty optimization the input-uncertainties of the velocity, of the cross-

sectional area and the traverse system have to be reduced.

3.5. Experimental validation of the quantified uncertainties

To validate the proposed uncertainty quantifications, the velocity–area methods were applied to the measurement data for all studied Reynolds numbers. As before five radial positions were considered. The velocity values for the recommended positions were calculated by an Akima-spline interpolation [6] of the measured 21 radial samples. As the positions are very close to the measured ones, the error caused by the interpolation is negligible. The calculated volume flows were compared to the flow rate values of the gravimetric flow meter standard. The derived errors are in the estimated scope. While C and CW show a relative difference of more than 1%, the methods LL and LC are in the range of 0.75–1%. The error of the flow rate determined with the optimized (opt) velocity–area method is lower than 0.3%, compare Fig. 8. The errors of the experimentally applied methods are within the estimated uncertainties that were evaluated for the LC and the optimized velocity area method, compare Table 1.

4. Conclusion

In the first step, existing velocity–area methods were applied to the theoretical profile from Gersten [8] representing fully developed pipe flow. An uncertainty quantification was derived. In the next step, a Reynolds number dependent theoretical model was derived from simulations and measurements in a Venturi nozzle. Applied to that *tanh* shaped profile, it was shown that the discretization error of the existing velocity–area methods is greater than 0.5%. To decrease the combined uncertainty, new measurement points were presented. These reduce the discretization error for the Venturi profile to 0.07%, in the Reynolds number interval $1 \times 10^5 - 1 \times 10^6$. Furthermore, the combined uncertainties concerning the flow rate are tabulated as an example for five radial sample positions. Due to the optimized sample positions for the nozzle profile, the overall uncertainty is reduced by 50%. The evaluated uncertainties were experimentally validated by comparison with a gravimetric flow meter standard.

The advantage of measuring in a Venturi nozzle is that the profile is stable and only slightly affected by upstream disturbances. Nonetheless, the stability of the profile inside the nozzle for asymmetric and swirl containing inflow has to be studied and incorporated in a future uncertainty evaluation.

References

[1] W. Aichelen, Der geometrische Ort für die mittlere Geschwindigkeit bei turbulenter Strömung in glatten und rauhen Rohren. Zeitschrift für Naturforschung 2a, (1947) 108–110, Online, ⟨http://www.degruyter.com/view/j/zna.1947.2.issue-2/zna-1947-0209/zna-1947-0209.xml⟩(accessed 14.04.14).
[2] ISO/TC 30/SC 2, DIN-EN-ISO-5167-3: Durchflussmessung von Fluiden mit Drosselgeräten in voll durchströmten Leitungen mit Kreisquerschnitt—Teil 3: Düsen und Venturidüsen, DIN Standard 2004.
[3] ISO/TC 30/SC 5, ISO 3354: Measurement of Clean Water Flow in closed

Conduits—Velocity–Area Method Using Current Meters in Full Conduits and Under Regular Flow Conditions, ISO Standard 2008.

[4] ISO/TC 30/SC 5, ISO 3966: Measurement of Fluid Flow in Closed Conduits—Velocity Area Method Using Pitot Static Tubes, ISO Standard 2008.

[5] Joint Committee for Guides in Metrology, Evaluation of Measurement Data—Guide to the Expression of Uncertainty in Measurement (GUM), Online, ⟨http://www.bipm.org/utils/common/documents/jcgm/JCGM_100_2008_E.pdf⟩, 2008 (accessed 29.04.15).

[6] E. Jones, T. Oliphant, P. Peterson, et al., SciPy-Open Source Scientific Tools for Python, Online, ⟨http://docs.scipy.org/doc/scipy-0.14.0/reference/generated/scipy.interpolate.Akima1DInterpolator.html⟩, 2001 (accessed 29.04.15).

[7] N. Mathies, Messunsicherheit einer gravimetrischen Kalt- und Warmwasser-Normalmessanlage für große Volumenströme (Ph.D. thesis), 2005, ISBN 3-86664-005-6.

[8] W. Merzkirch, et al., Fluid Mechanics of Flow Metering, Springer-Verlag, 2005 http://www.springer.com/materials/mechanics/book/978-3-540-22242-2.

[9] R.W. Miller, Flow Measurement Engineering Handbook, McGraw-Hill Book Company, 1983, ISBN 0-07-042045-9.

[10] John.A. Nelder, R. Mead, A simplex method for function minimization, Comput. J. 7 (1965) 303–313, Online, http://comjnl.oxfordjournals.org/cgi/reprint/7/4/308.pdf (accessed 19.03.15).

[11] V. Strunck, B. Mickan, N. Pape, H. Müller, Durchflussmessung am optischen Normal für Erdgas unter Hochdruck. Fachtagung "Lasermethoden in der Strömungsmesstechnik" 19, Online, ⟨http://www.gala-ev.org/images/Beitraege/Beitraege%202011/pdf/Nr_p13.pdf⟩, 2011 (accessed 14.04.14).

[12] VDI/VDE, VDI 2640—Blatt 1: Netzmessung in Strömungsquerschnitten - Allgemeine Richtlinien und mathematische Grundlagen, VDI/VDE Standard, 1993.

[13] A. Weissenbrunner, T. Eichler, T. Lederer, Simulation einer 7% Segmentblende und Vergleich mit PIV-Messungen, Fachtagung "Lasermethoden in der Strömungsmesstechnik" 22, Online, ⟨http://www.gala-ev.org/images/Beitraege/Beitraege%202014/pdf/22.pdf⟩, 2014 (accessed 16.03.15).

[14] D.C. Wilcox, Multiscale model for turbulent flows. AIAA JOURNAL 26, Online, ⟨http://arc.aiaa.org/doi/abs/10.2514/3.10042⟩, 1988 (accessed 29.04.15).

[15] F. Winternitz, C. Fischl, A simplified integration technique for pipe-flow measurement, Water Power (1957) 225–234.